Numerical Analysis of Neutron Moisture Probe Measurements

Jie Li[1]; David W. Smith[2]; Stephen G. Fityus[3]; and Daichao Sheng[4]

Abstract: The neutron probe has proven to be an effective means for monitoring long term in situ soil moisture variations. However, it is difficult to experimentally correlate neutron probe data (i.e., neutron counts) with accurate estimates of absolute soil moisture content, particularly for unsaturated clay soils. In this paper, a numerical model based on multigroup neutron diffusion theory is employed to predict the distribution of neutron flux in a neutron probe system. The model discretizes the neutron energy spectrum into seven intervals, with energy-dependent diffusion coefficients and parameters for each energy interval. The finite element method is employed to solve the coupled seven-group neutron diffusion equations. It is demonstrated that the numerical results compare very well with both laboratory experimental results and field measurements. The theoretical approach to neutron probe calibration described herein offers significant time and cost savings over traditional calibration methods, and potentially opens up new applications for neutron probe monitoring.

DOI: 10.1061/(ASCE)1532-3641(2003)3:1(11)

CE Database subject headings: Calibration; Soil moisture; Finite element method; Numerical analysis; Measurement.

Introduction

The neutron-scattering method is widely used in agriculture, forestry, hydrology, and civil engineering, for measuring the water content of soil. The main advantages of the neutron method compared to the gravimetric method are (1) it is nondestructive, (2) it is fast, and (3) repeated measurements can be carried out in situ.

Although the neutron probe has proven to be a convenient and effective means for monitoring long-term in situ soil moisture variations (Schmugge et al. 1980; Silvestri et al. 1991), the experimental correlation of neutron probe data (i.e., neutron counts) with moisture contents to give accurate absolute values of moisture content is a difficult task, particularly for clay soils. Neutron probe counts in moist soils are influenced by the moisture content, soil elemental composition, soil density, and proximity of the probe to the water table and soil surface (Dickey 1990). Neutron counts are also influenced by the strength of the neutron source, the size and type of the neutron detector, the position of the detector relative to the source, and the size and type of access tube (Schmugge et al. 1980; Stone 1990). It has been shown that factory calibrations are often inaccurate (see, for example, Bell and McCulloch 1969; Rawls and Asmussen 1973; Vachaud et al. 1977; Carneiro and Jong 1985; Chanasyk and Naeth 1996). For example, Silvestri et al. (1991) found that the factory calibration curve supplied by the manufacturer was only applicable for sandy soil (with no significant amount of absorbing elements or organic materials), and only for volumetric water contents ranging from 0 to 33%. Calibration is therefore necessary for each type of soil, different types of access tube, and different measuring locations with respect to the soil surface and water table.

Calibration of a neutron probe involves correlating neutron counts with known volumetric water contents of the soil. Two experimental approaches are commonly employed: laboratory drum calibration, and in situ or field calibration. Laboratory calibrations are made by packing a drum of suitable dimensions with the soil having a range of known moisture contents, installing an access tube as used in the field, and measuring the neutron probe counts. The radius of the drum must be larger than the radius of influence of the neutron probe to prevent neutron leakage. The soil used in laboratory calibrations should have the same elemental composition and bulk density as the soil in the field. However, it is usually difficult to reproduce in a drum the soil fabric found in situ (IAEA 1970).

Field calibrations are accomplished by correlating the probe readings in an access tube installed in the field, with the estimated volumetric moisture contents of the soil along the tube (or possibly immediately adjacent to the tube). These comparisons have to be repeated at different times of the year, so as to sample the soil at different moisture contents. The volumetric moisture contents are usually estimated from gravimetric soil moisture content and soil density. However, it is often difficult to obtain representative soil samples from heterogeneous soil profiles. In addition, the soil moisture content in the field may vary rapidly with depth, significantly complicating the interpretation of neutron readings. Detailed descriptions of the laboratory and field calibrations can be found in Greacen (1981) and IAEA (1970).

Even though both laboratory and field calibrations are time consuming and labor-intensive, the results are not always satisfactory, especially for clay soils. Greacen (1981) indicated that early ''calibration curves for clay soils'' in the literature were

[1]Dept. of Civil, Surveying and Environmental Engineering, Univ. of Newcastle, Callaghan, NSW 2308, Australia. E-mail: jlie@mail.newcastle.edu.au

[2]Dept. of Civil, Surveying and Environmental Engineering, Univ. of Newcastle, Callaghan, NSW 2308, Australia.

[3]Dept. of Civil, Surveying and Environmental Engineering, Univ. of Newcastle, Callaghan, NSW 2308, Australia.

[4]Dept. of Civil, Surveying and Environmental Engineering, Univ. of Newcastle, Callaghan, NSW 2308, Australia.

Note. Discussion open until February 1, 2004. Separate discussions must be submitted for individual papers. To extend the closing date by one month, a written request must be filed with the ASCE Managing Editor. The manuscript for this paper was submitted for review and possible publication on November 14, 2001; approved on March 5, 2002. This paper is part of the ***International Journal of Geomechanics***, Vol. 3, No. 1, September 1, 2003. ©ASCE, ISSN 1532-3641/2003/1-11–20/$18.00.

''almost invariably wrong.'' The problem is further complicated for unsaturated expansive clay soils, due to the fact that both soil volume and density change as the in situ soil moisture content changes. Experimental investigations on various types of soil have shown that, in addition to the moisture content, the neutron probe reading depends mainly upon the dry bulk density of the soil (IAEA 1970).

In some circumstances, it is nearly impossible to obtain an experimental calibration. Morris and Williams (1990) discussed the attempted neutron probe calibration of fine-grained coal mine tailings first deposited as a slurry, and then sedimented and finally consolidated. They found that it was impractical to directly measure density profiles with depth as the majority of the tailings were too soft to sample. In another example, Elder and Rasmussen (1994) reported that the experimental calibrations were unsuitable for some geologic media, such as unsaturated tuff, due to the difficulty of extracting undisturbed samples for volumetric moisture content measurement.

Because the neutron probes can be so difficult to calibrate by experimental methods, it is desirable to develop an alternative and more reliable calibration method. The purpose of this study is to develop a generalized calibration method from first principles that can be used for all media. The method is based on a numerical model of the neutron probe system and on the elemental composition of the medium in which the neutron probe is used. The theory behind the model is known as ''multigroup neutron diffusion theory'' (Isbin 1963; Zweifel 1973; Iliffe 1982; Stacey 2001). The numerical model predicts the count rate for a neutron probe based on dry density, moisture content, and elemental composition of the soil, and the known geometry and size of the neutron detector and source, and strength of the neutron source.

Theoretical Background

Physical Phenomena Involved in Neutron Moisture Gauges

The neutron moisture gauge consists of a probe containing a source of fast (high-energy) neutrons that move radially outward from the source, a thermal neutron detector, and the associated electronic equipment necessary to supply power for the detector and to display the results. A gauge is illustrated in Fig. 1. Measurements with depth are made by lowering the probe down an access tube, usually made of either stainless steel or aluminum, to the required depths of measurement. Aluminum is generally the material of choice because it has the low absorption cross section for slow (thermalized) neutrons. Stainless steel tubes may have to be used if the soil is corrosive.

The neutron scattering method for measuring soil water content exploits neutron ''thermalization behavior.'' When the neutron probe is in the borehole, fast neutrons emitted by the source collide with the atomic nuclei of the surrounding medium. Each collision between a neutron and a nucleus results in a transfer of energy from the neutron to the nucleus. The average energy decrement per collision (ξ) is defined as (Glasstone and Edlund 1957; Weinberg and Wigner 1958)

$$\xi = 1 + \frac{(A-1)^2}{2A} \ln \frac{A-1}{A+1} \tag{1}$$

where A = atomic mass of the impacted nucleus.

It can be seen from Eq. (1) that ξ is dependent only on the atomic mass of the impacted nucleus, and is independent of the initial energy of the neutrons. In other words, after each collision, the neutron always loses the same fraction of its energy. This fraction decreases with increasing atomic mass of the impacted nucleus. Using ξ, the average number of collisions required to convert fast neutrons with initial energy of E_0, say, two million electron volts (MeV), to the thermal value of $E = 0.025$ electron volts (eV), can be calculated as follows (Glasstone and Edlund 1957; Gibson 1980):

$$\begin{aligned} &\text{Average number of collisions to thermalize} \\ &\text{fast neutrons (from 2 MeV to 0.025 eV)} \\ &= \frac{\ln \frac{E_0}{E}}{\xi} = \frac{\ln \frac{2 \times 10^6}{0.025}}{\xi} = \frac{18.2}{\xi} \end{aligned} \tag{2}$$

The results of a set of these calculations for a number of selected elements are given in Table 1. From the table, it can be seen that

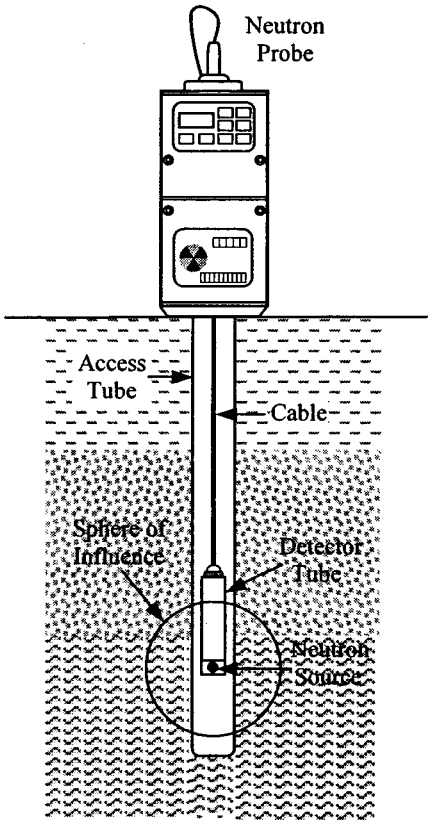

Fig. 1. Schematic of neutron gauge

Table 1. Number of Collisions Required to Thermalize a Fast Neutron for Selected Elements

Element	Atomic mass	ξ	Number of collisions
Hydrogen	1.008	1.00000	18
Deuterium	2.000	0.72500	25
Helium	4.003	0.42500	43
Lithium	6.940	0.26200	69
Beryllium	9.013	0.20600	88
Carbon	12.011	0.15800	115
Oxygen	16.000	0.12000	152
Sodium	22.991	0.08500	215
Iron	22.850	0.35400	514
Uranium	238.070	0.00838	2,172

hydrogen nuclei have a much greater thermalizing effect on fast neutrons than any other element. Since neutrons and hydrogen atoms have the same mass, fast neutrons are slowed down most effectively by collisions with hydrogen atoms, much like a billiard ball hitting a stationary ball of the same size and each moving away with equal speeds (one slowing down and the other speeding up). This is the fundamental reason why a neutron gauge can be employed to detect the proportion of water molecules present in a soil.

Neutron Sources

The radioisotope most commonly employed in moisture gauges is Americium-241. Americium undergoes decay to Neptunium, ejecting an alpha particle in the process. Beryllium, which is incorporated in the source, is bombarded by α particles and converted into carbon and ''fast neutrons,'' according to the reaction

$$^{9}_{4}\mathrm{B}_{e}+^{4}_{2}\mathrm{H}_{e}\rightarrow^{1}_{0}n+^{12}_{6}\mathrm{C} \tag{3}$$

Most neutron probes also emit a low level of γ radiation. γ rays may arise from the radioisotope itself or from $^{12}_{6}$C left in the excited state after conversion from beryllium (IAEA 1970). At present, the most widely used neutron source is ^{241}Am-Be because it produces a much lower level of γ radiation than a ^{226}Ra-Be source, and so needs very little shielding. With a half life of approximately 460 years, the ^{241}Am-Be source can be permanently sealed in a shielded container and maintain an effectively constant neutron production rate for many years.

Neutron Energy Spectrum

The fast neutrons from the radioactive source in a neutron probe possess a range of velocities and energies. For example, fast neutrons emitted from an Americium-241-Beryllium source have an initial energy of approximately 4.5 MeV. As the fast neutrons diffuse in the soil medium, they are slowed down and lose energy, mainly by elastic collisions with hydrogen nuclei (and to a lesser extent by absorption), and finally become ''thermalized.'' Thermalization is the process whereby neutrons are slowed to the point where further collisions with hydrogen and other materials do not continue to slow the neutrons further (i.e., they are just as likely to gain energy as lose energy in collisions once thermalized).

It is important to note that neutron transport involves a spectrum of energy levels, scattering collisions, and absorption reactions (see next section). Fast neutrons are defined here as those having kinetic energies in excess of 2 eV, while slow neutrons are defined as those with kinetic energy below 2 eV. It should be noted that the slow neutrons may be further divided into two groups: ''thermal neutrons'' having energies from 0 to 0.5 eV, and so-called ''epithermal neutrons'' with energies between 0.5 and 2.0 eV (IAEA 1970).

Neutron Interactions and Cross Sections

Neutron interactions with the surrounding material can be classified as either absorption reactions or scattering interactions. Absorption is the process where a neutron enters a nucleus, thereby forming a new isotope in an excited state, which usually rapidly relaxes by emitting gamma radiation. Absorption reactions are strongly dependent on the neutron energy level. The absorption of fast neutrons can usually be neglected in ordinary soils since absorption rapidly decreases for energies above the thermal range.

In scattering interactions, the kinetic energy of a neutron is partially or completely transferred to the impacted nuclei in successive collisions through elastic or inelastic scattering. Reactions due to elastic scattering are by far the dominant mode of interaction of fast neutrons in soils (IAEA 1970).

Neutron interactions with atomic nuclei (whether scattering or absorption), can be quantitatively described through the use of the concept of *nuclear cross sections*. A cross section is defined as the probability of occurrence of a given type of nuclear interaction. The experimental determination of cross sections is based on the attenuation of a collimated neutron beam passing through a slab of material of finite thickness. Defining d as the distance through the slab in the direction of the beam, the number of neutrons varies with distance through the slab according to

$$I=I_{0}e^{-\Sigma d} \tag{4}$$

where I_0 = initial neutron intensity; I = neutron intensity at distance d; and Σ is called the ''macroscopic cross section.'' The units of Σ are inverse length (usually cm^{-1}), because the exponent (Σd) has no dimension. The ''microscopic cross section'' denoted (σ) is obtained by dividing Σ by the number of element nuclei per unit volume, so σ has units of area. The unit usually used to describe nuclear reaction cross sections is the *barn*; one barn defined as 10^{-24} cm^2.

The general equation describing the macroscopic cross section for a soil containing n different elements is

$$\sum =N_{1}\sigma_{1}+N_{2}\sigma_{2}+\cdots=\sum_{i=1}^{n}N_{i}\sigma_{i} \tag{5}$$

where N_i = number of atoms of element i per cm^3 of the medium and σ_i = its microscopic cross section at the specified energy level (and for the specified interaction; the designations σ_s and σ_a are used for scattering and absorption interactions, respectively). With Avogadro's number ($N_0=6.02\times10^{23}$), Eq. (5) can be rewritten more conveniently as

$$\sum =6.02\times10^{-3}\rho\sum_{i=1}^{n}\frac{w_{i}\sigma_{i}}{A_{i}} \tag{6}$$

where A_i = atomic weight of the ith element (see Table 2); w_i = percentage weight of the ith element; and ρ = density of the medium in g/cm^3.

In practically every case known, the microscopic cross section (σ) depends on the energy level of the neutrons. To illustrate this, the microscopic elastic scattering cross sections for hydrogen and oxygen are shown in Fig. 2. For these elements, elastic scattering cross sections are almost constant over the middle energy levels, but decrease at higher neutron energies (and may vary irregularly; see for example, oxygen), while at low energies scattering usually increases.

As noted previously, the absorption of fast neutrons can usually be neglected in ordinary soils since absorption rapidly decreases for energies above the thermal range. At low energy levels, absorption is approximately inversely related to the neutron velocity (i.e., σ_a is proportional to $1/v$). This behavior is often referred to as the ''$1/v$ law'' (Iliffe 1982).

The theoretical determination of nuclear cross sections for scattering and absorption interactions is a complex problem, and so the cross sections are usually measured experimentally. A list of microscopic thermal absorption and microscopic scattering cross sections of the 20 most common elements in most soils is shown in Table 2 [data for other elements can be found in Stacey

Table 2. Microscopic Thermal Cross Sections (from Stacey 2001)

Element	Atomic mass A	$\sigma_a^{2,200}$ barn	$\overline{\sigma_s}$ barn
H	1.008	0.33200	20.49[a]
Li	6.940	71.00000	1.40
B	10.820	755.00000	4.00
C	12.011	0.00373	4.80
N	14.008	1.88000	10.00
O	16.000	0.00020	4.20
Na	22.990	0.50500	4.00
Mg	24.320	0.06900	3.60
Al	26.980	0.24100	1.40
Si	28.090	0.16000	1.70
P	30.975	0.20000	5.00
S	32.066	0.52000	1.10
Cl	35.457	33.80000	16.00
K	39.100	2.07000	1.50
Ca	40.080	0.44000	3.00
Ti	47.900	5.80000	4.00
Mn	54.940	13.20000	2.30
Fe	55.850	2.62000	11.00
Co	58.940	38.00000	7.00
Cd	112.410	2,450.00000	7.00
H_2O	18.016	0.66400	—

[a]From Mughabghab et al. (1981).

(2001)]. The 2,200 superscript represents the neutron velocity (v) when thermalized (i.e., at 0.025 eV, $v = 2{,}200$ m/s).

Neutron Flux

The ''neutron flux'' ϕ is a very significant quantity in all studies concerning neutrons. For a prescribed energy level it is defined as (Glasstone and Edlund 1957)

$$\phi = nv \tag{7}$$

where n = neutron density (i.e., the number of neutrons per cubic centimeter) and v = neutron velocity (e.g., cm/s). Hence the units of neutron flux are (neutrons)(cm)/(cm^3)(s), that is, neutrons/cm^2-s (as is suggested by the name ''neutron flux''). However, one should not be misled by the usual interpretation that the flux represents the number of neutrons crossing a unit area per unit time. This interpretation is correct only for a collimated beam (all neutrons traveling in one direction) with the unit area taken normal to the travel direction. In a neutron gauge system, the neutrons may travel in all directions. The general interpretation of the flux is that the product, nv, represents the sum of the distances traveled by all the neutrons in one second in a unit volume. This interpretation is independent of neutron direction.

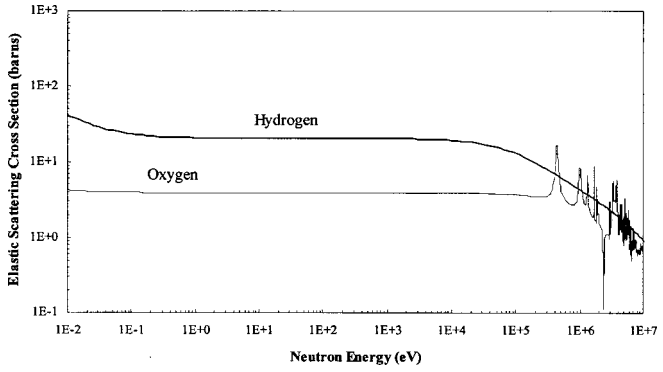

Fig. 2. Elastic scattering cross section of $^1H_1$ and $^{16}O_8$ as function of neutron energy after Stacey (2001)

Since neutron cross sections are energy-dependent, the neutron flux is often expressed as a function of energy. The total flux over the energy range E_1 to E_2 is then

$$\phi = \int_{E_1}^{E_2} n(E)v(E)dE = \int_{E_1}^{E_2} \phi(E)dE \tag{8}$$

where $n(E)$ defines the number of neutrons per unit volume *per unit energy interval*. Hence $n(E)dE$ is the number of neutrons per unit volume in the energy interval from E to $E+dE$.

Neutron Current

Another important quantity for describing neutron behavior is the neutron current $\boldsymbol{J}$ (also known as neutron current density). Using Fick's law of diffusion, the net current of monoenergetic neutrons (i.e., neutrons of uniform energy) can be written as (Isbin 1963; Stacey 2001)

$$\boldsymbol{J} = -D \ \text{grad} \ \phi \tag{9}$$

where the neutron current vector $\boldsymbol{J}$ = net number of neutrons flowing in a given direction in unit time through a unit area normal to the direction of flow and D = diffusion coefficient.

It should be noted that the units of neutron flux and neutron current are the same (neutrons per square centimeter per second), but the neutron current is a vector quantity, while the neutron flux is a scalar quantity. Eq. (9) then implies that the diffusion coefficient has units of length (cm). When the energy spectrum of the neutrons is considered, the neutron current becomes a function of the energy, as does the neutron flux (ϕ) and neutron density (n).

Neutron Diffusion Equation

When neutrons have slowed to thermal energies, their spatial movement is quite similar to the diffusion of gases, except that their lifetime is limited by absorption (IAEA 1970). After high-energy neutrons are emitted by the source and diffuse outward through the soil, a fraction of the slow neutrons rebound back towards the probe and are absorbed by the nucleus of the gas in the detector, giving rise to a signal that, after processing, is known as the ''neutron count.'' The detector only measures slow neutrons.

It can be summarized that in a neutron moisture probe the fast, high-energy neutrons emitted from the source undergo simultaneously the processes of transport (diffusion) and slowing-down (themalization). Therefore a model describing neutron moisture probe behaviors must take into account the complete energy spectrum of neutrons, from their initial fast state to their thermalized state. A straightforward and practical approach is to subdivide the continuous energy spectrum of all neutrons into a number of discrete energy groups so that each energy group can, to reasonable approximation, be treated as monoenergetic with constant parameters. A set of simultaneous diffusion equations then covers the whole neutron spectrum from fast down to thermal, a representation known as ''multigroup diffusion theory'' (Iliffe 1982).

For a given neutron energy group, the neutron balance (or conservation) equation under steady-state conditions is expressed as:

$$\overbrace{(-\nabla \boldsymbol{J})}^{\text{Leakage}} + \overbrace{(\Sigma_{\text{sl}_i}\phi_i + \Sigma_{a_i}\phi_i)}^{\text{Sink}} = \overbrace{(S \ \text{ or } \ \Sigma_{\text{sl}_{i-1}}\phi_{i-1})}^{\text{Source}} \tag{10}$$

From this neutron balance, the neutron diffusion equation for an n-group diffusion model can be written in the form

$$\left.\begin{array}{ll} D_1\nabla^2\phi_1-\Sigma_{sl_1}\phi_1-\Sigma_{a_1}\phi_1+S=0 & E_1\geq E>E_2 \\ D_2\nabla^2\phi_2+\Sigma_{sl_1}\phi_1-\Sigma_{sl_2}\phi_2-\Sigma_{a_2}\phi_2=0 & E_2\geq E>E_3 \\ D_3\nabla^2\phi_3+\Sigma_{sl_2}\phi_2-\Sigma_{sl_3}\phi_3-\Sigma_{a_3}\phi_3=0 & E_3\geq E>E_4 \\ \cdots\ \cdots \qquad \cdots\cdots & \\ D_n\nabla^2\phi_n+\Sigma_{sl_{n-1}}\phi_{n-1}-\Sigma_{a_n}\phi_n=0 & E_n\geq E \end{array}\right\} \tag{11}$$

where S = high-energy neutron source term; D_i = diffusion coefficient for the ith energy group; Σ_{sl_i} = slow-down cross section; Σ_{a_i} = macroscopic absorption cross section; and E_i = energy interval. The unknown quantities ϕ_1, are the neutron flux fields to be found [defined in Eq. (8)]. The groups are numbered from 1, for the highest energy, to n, for the lowest (i.e., thermal) energy. Clearly the larger the number of energy groups, the greater the accuracy, since one is attempting to represent the actual continuous energy distribution in a material by a finite number of discrete groups. In an index notation, Eqs. (11) are denoted

$$\frac{\partial}{\partial x_i}\left(D_{lk}\frac{\partial\phi_k}{\partial x_i}\right)-a_{lk}\phi_k=-f_l \tag{12}$$

where the standard summation convention applies. a_{lk} = matrix of the slow-down and absorption cross sections. It is noted that the diffusion coefficient in Eq. (12) represents a constant (i.e., for an isotropic material), and is not a second order tensor quantity.

In its crudest approximation, ''multigroup diffusion theory'' reduces to a single group. Single group theory assumes that all diffusion and absorption of neutrons occur in a single energy, that is, at the thermal energy. Obviously, this model is not a good model for neutron probe analysis. The two-group diffusion model breaks the energy spectrum of neutrons into two separate groups (i.e., fast and thermal groups), while for the three-group theory, the fast neutrons are further split into an upper and lower fast groups. Analytical solutions to Eq. (11) or (12) are available for one-, two- and three-group diffusion theory, assuming a point source situated in an infinite homogeneous medium.

Two-group theory was used by Haahr and Olgaard (1965) to determine a so-called ''sphere of importance.'' Olgaard (1965) also used three-group diffusion theory as an improvement on the two-group theory calculations and achieved reasonable agreement with some experimental measurements in various soil types. Based on the three-group model developed by Olgaard (1965), Elder and Rasmussen (1994) obtained a calibration equation between neutron counts and water content in an unsaturated tuff. The three-group approximation was also applied by Morris and William (1990) to develop a moisture content calibration for coal mine tailings.

While these solutions have served to assist in neutron probe calibration, the assumptions made in deriving the analytic solutions clearly ignore the access tube geometry, probe and detector geometry, the spatially variable soil composition, and the boundary conditions encountered in practice.

In this study, a numerical model based on seven-group diffusion theory has been developed to give a better physical description of the problem and to improve upon previous results. Seven-group diffusion theory (whose upper and lower energy limits are given in Table 3), was found to be sufficiently accurate to describe neutron slowing down and diffusion in a neutron gauge. As far as the writers are aware, this is the first time a seven-group diffusion theory has been applied to a neutron probe analysis.

Table 3. Upper and Lower Energy Limits E_i Used in Numerical Model

Group	Upper limit	Lower limit
1	4.5 MeV	4.0 MeV
2	4.0 MeV	3.0 MeV
3	3.0 MeV	2.0 MeV
4	2.0 MeV	1.0 MeV
5	1.0 MeV	0.1 MeV
6	0.1 MeV	1.44 eV
7	1.44 eV	$5kT_n$[a] eV

[a] T_n is the neutron temperature.

Calculation of Diffusion Coefficient, Slow-down, and Absorption Cross Sections

To solve the neutron diffusion Eq. (11), the diffusion coefficients D_i, the slow-down cross sections Σ_{sl_i}, and the absorption cross section Σ_{a_i} have to be first estimated. As mentioned previously, absorption rapidly decreases for energies above the thermal energy. Therefore absorption of fast neutrons can be neglected in moisture gauge studies with little loss in accuracy.

By assuming that the thermal neutrons are distributed according to the Maxwell-Boltzmann distribution law (because the thermal neutrons behave like an ideal gas) and that all absorbers follow the ''1/v law,'' then the absorption cross section for the thermal neutrons is found to be (Olgaard 1965)

$$\Sigma_a=\frac{\sqrt{\pi}}{2}\Sigma_a^{2,200}\sqrt{\frac{293}{T_n}} \tag{13}$$

where $\Sigma_a^{2,200}$ and T_n = total macroscopic absorption cross section of the medium corresponding to a neutron velocity of 2,200 m/sec and the neutron temperature, respectively. T_n is obtained from the following relation (Weinberg and Wigner 1958):

$$T_n=T_m\left(1+0.92\frac{\Sigma_a^{2,200}}{\bar{\Sigma}_s/A}\sqrt{\frac{293}{T_m}}\right) \tag{14}$$

It can be seen that the neutron temperature is always higher than the physical temperature, T_m (in °K), of the medium in which neutrons diffuse, and this difference is dependent on the macroscopic absorption cross section of the medium. $\Sigma_a^{2,200}$ may be calculated based on the experimentally estimated microscopic cross sections given in Table 2, viz,

$$\Sigma_a^{2,200}=n_{H_2O}\sigma_{a,H_2O}^{2,200}+\sum_1^n n_i\sigma_{a,i}^{2,200} \tag{15}$$

where n_i and n_{H_2O} = number of atoms of a specific chemical element and the number of water molecules per cubic centimeter respectively. n_i is defined as

$$n_i=\frac{6.02\times10^{23}}{A_i}\times\rho_s\times\frac{w_i}{100} \tag{16}$$

where ρ_s = dry density of the soil and A_i = atomic mass given in Table 2. The mass percentage of the ith element w_i is usually determined from the chemical analysis of the soil material. If the volume fraction of water in the soil (in percent of the total volume) is equal to V_w, n_{H_2O} is given by (Olgaard 1965)

$$n_{H_2O} = \frac{6.02\times 10^{23}}{18.016}\times \rho_w \times \frac{V_w}{100} \quad (17)$$

The density of water ρ_w shown in Eq. (17) is a function of water temperature t_m in degrees centigrade. This relationship is taken to be

$$\rho_w = 0.9998 + 6.296\times 10^{-5} t_m - 8.201\times 10^{-6} t_m^2 + 4.826\times 10^{-3} t_m^3 \quad (18)$$

For the calculation of the thermal neutron temperature [Eq. (14)], a value of Σ_s/A may be estimated using the following formula

$$\Sigma_s/A = n_{H_2O}(2\overline{\sigma}_{s,H}/A_H + \overline{\sigma}_{s,O}/A_O) + \sum_1^n n_i \overline{\sigma}_{s,i}/A_i \quad (19)$$

For thermalized neutrons, both the macroscopic scattering and absorption cross sections are important. The macroscopic thermal scattering cross sections of the soil elements are calculated with the assumption that the microscopic scattering cross sections of all elements in the material are independent of neutron energy; but the contribution to $\Sigma_s(1-\overline{\mu})$ from water is assumed to be dependent on the neutron temperature [see Eq. (20)]. This is expressed by

$$\Sigma_s(1-\overline{\mu}) = 2.156\times \left(0.047 + 0.953\sqrt{\frac{293}{T_n}}\right)\times \rho_w \frac{\nu_w}{100} + \sum_1^n n_i \overline{\sigma}_{s,i}\left(1-\frac{2}{3A_i}\right) \quad (20)$$

Once the macroscopic absorption and scattering cross sections have been determined, the macroscopic transport cross section of the medium Σ_{tr} and the thermal diffusion coefficient D_{th} are calculated using (IAEA 1970)

$$\Sigma_{tr} = \Sigma_s(1-\overline{\mu}) + \Sigma_a \quad (21)$$

$$D_{th} = \frac{1}{3\Sigma_{tr}} \quad (22)$$

For fast neutrons, the scattering interaction is of primary importance (i.e., absorption is small and so neglected). The slow-down cross sections are determined using (Iliffe 1982)

$$\Sigma_{sl_i} = \frac{(\xi\Sigma_s)_i}{\ln(E_i/E_{i+1})} \quad (23)$$

The product $\xi\Sigma_s$ is called the ''macroscopic slowing down power'' and given by

$$(\xi\Sigma_s)_i = n_{H_2O}[2(\overline{\xi}\overline{\sigma}_s)_{H,i} + (\overline{\xi}\overline{\sigma}_s)_{O,i}] + \sum_{j=1}^n n_i(\overline{\xi}\overline{\sigma}_s)_{j,i} \quad (24)$$

where Σ_{s_i} = macroscopic cross section for scattering. Considering the forward biases from the ''center of mass correction'' and the anisotropic scattering, the energy-dependent expressions for $\overline{\xi}$ and $\overline{\mu}$ are taken to be (Weinberg and Wigner 1958)
for $0.07A^{2/3} \leqslant 0.2$

$$\overline{\mu} = \frac{2}{3A} + 0.07A^{2/3}E\left(1-\frac{3}{5A^2}\right) \quad (25)$$

$$\overline{\xi} = \xi - 0.21A^{2/3}E\times\left(\frac{\xi}{a}-0.5\right) \quad (26)$$

for $0.07A^{2/3} > 0.2$

$$\overline{\mu} = \frac{2}{3A} + 0.2\left(1-\frac{3}{5A^2}\right) \quad (27)$$

$$\overline{\xi} = \xi - 0.6\times\left(\frac{\xi}{a}-0.5\right) \quad (28)$$

Fast group constants Σ_{tr} and D_i are now obtained from

$$\Sigma_{tr} = [\Sigma_s(1-\overline{\mu})]_i = n_{H_2O}\{2[\sigma_s(1-\overline{\mu})]_{H,i} + [\sigma_s(1-\overline{\mu})]_{O,i}\} + \sum_{j=1}^n n_i[\sigma_s(1-\overline{\mu})]_{j,i} \quad (29)$$

$$D_i = \frac{1}{3\Sigma_{tr}} \quad (30)$$

The fast microscopic scattering cross sections (σ_s) for each energy group, can be estimated using the figures in Hughes and Schwartz (1958) or Mughabghab et al. (1981). As noted previously and from the cross-section curves given in Hughes and Schwartz (1958), it can be seen that the cross sections for fast neutrons may vary in a highly irregular way with energy level, having many high sharp peaks. If required, more accurate cross-section data can be obtained from the *MIRANDA* code developed by the Australian Nuclear Science and Technology Organization (Robinson and Harrington 1998), which contains the cross-section library for all elements over the 200 energy groups (covering the range 15.5 MeV to 1×10^{-5} eV) based on the U.S. data file *ENDF/B-VI*.

Material Interface and Boundary Conditions

In order to solve the general governing Eq. (11) or (12), the following material interface and boundary conditions need to be specified.

Interface Between Two Different Mediums

At an interface between two media with different diffusion properties (for example, between the detector and soil or between two different soils), both neutron flux and neutron net current must be continuous across the interface. If two media are denoted by the symbols *A* and *B*, then the required boundary conditions for neutrons with a particular energy range are simply,

$$\phi_A = \phi_B \quad (31)$$

$$\boldsymbol{J}_A = \boldsymbol{J}_B \quad (32)$$

Soil-Atmosphere Boundary

At the top surface of a soil profile, there is a flow of neutrons out of the surface but there is practically no flow from the atmosphere back into the surface. The correct boundary condition is clearly that there are no neutrons returned from the atmosphere to the soil (Fig. 3). Generally, the net neutron current $\boldsymbol{J}$ represents the balance between the currents in the positive (outward) and negative (inward) directions; according to neutron diffusion theory these are defined as

$$J_{out}^{+} = \frac{\phi_i}{4} - \frac{1}{2}\vec{n}\cdot(D_i\nabla\phi_i) \quad (33)$$

$$J_{in}^{-} = \frac{\phi_i}{4} + \frac{1}{2}\vec{n}\cdot(D_i\nabla\phi_i) \quad (34)$$

where ϕ_i and D_i = neutron flux and the diffusion coefficient for the *i*th energy group, respectively. The difference between these

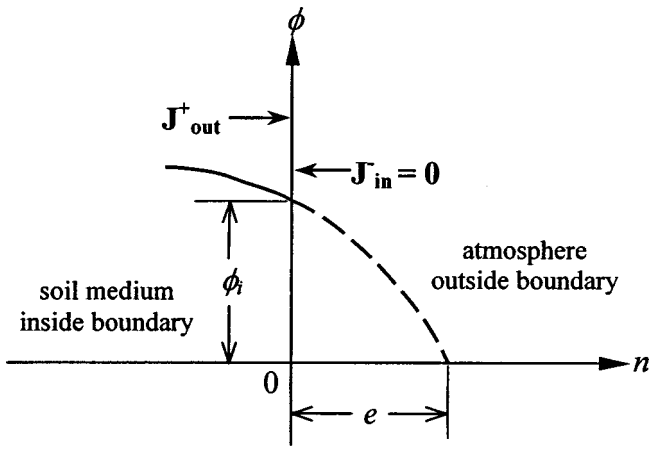

Fig. 3. Interface between soil and atmosphere

two components gives the net neutron current, in agreement with Eq. (9). Since there is no scattering back of neutrons from the air into the soil medium, the negative component of the neutron current for all seven energy groups is zero and so

$$J^-_{\text{in}} = \frac{\phi_i}{4} + \frac{1}{2}\vec{n}\cdot(D_i \nabla \phi_i) = 0 \tag{35}$$

Since the flux ϕ_i at the boundary is positive, the flux gradient $(\nabla\phi_i)$ must be negative, as indicated schematically in Fig. 3. Therefore if the neutron flux is extrapolated into the air, as shown in Fig. 3, it will vanish at some distance e beyond the boundary. It can be seen that modeling the response of a neutron gauge is a complex problem. Analytical solutions are possible only for the very simplest cases, and consequently numerical methods need to be adopted. Given that the problem geometry may be irregular, that there may be multiple materials with varying properties, and a range of different types of boundary conditions, it is apparent that solving the neutron diffusion equations is ideally suited to the finite element method.

Numerical Model

Finite Element Formulation

The governing differential equation for multigroup neutron diffusion with boundary conditions can be written as

$$\begin{aligned} &-\frac{\partial}{\partial x_i}\left(D_{lk}\frac{\partial \phi_k}{\partial x_i}\right) + a_{lk}\phi_k = f_l \quad \text{in } \Omega \\ &n_i\left(D_{lk}\frac{\partial \phi_k}{\partial x_i}\right) + q_{lk}\phi_k = g_l \quad \text{on } \partial\Omega \\ &h_{lk}\phi_k = r_l \quad \text{on } \partial\Omega \end{aligned} \tag{36}$$

where Ω = domain and $\partial\Omega$ = boundary of the domain. The second equation is referred to as a generalized Neumann boundary condition, and the third equation as a Dirichlet boundary condition. For two-dimensional or axisymmetric problems the space index i ranges from 1 to 2. The component indices k and l range from 1 to N; where N is the number of coupled second-order partial differential equations; and n_i is the ith component of the outward normal vector.

Eq. (36) is solved using the finite element spatial discretization procedure. Without restricting the generality, we assume generalized Neumann conditions on the whole boundary. Multiplying an arbitrary test function ν by Eq. (36) and applying Gauss's theorem, we find

$$\int_\Omega \left[\left(D_{lk}\frac{\partial \phi_k}{\partial x_i}\right)\frac{\partial \nu}{\partial x_i} + a_{lk}\phi_k\nu\right]dx + \int_{\partial\Omega} q_{lk}\phi_k\nu\, ds = \int_\Omega f_l\nu\, dx + \int_{\partial\Omega} g_l\nu\, ds \tag{37}$$

This equation defines the weak or variational form of the governing differential equation. Obviously, any solution of the differential equation is also a solution of the variational problem. In order to obtain the weak solution of Eq. (37), we need to project the weak form of the differential equation onto a finite dimensional function space (i.e., a set of continuous, piecewise linear functions on a triangulation τ of the domain Ω). Introducing the space discretization

$$\phi_k(x) \approx \sum_{I=1}^{N_p} \psi_{I,k} N_I(x) \tag{38}$$

where N_I = shape functions; $\psi_{I,k}$ = nodal values of the unknown; and N_p = number of nodes in an element. By setting the test functions ν equal to the shape function N_J in Eq. (37), we obtain a system of equations in matrix form as

$$(\boldsymbol{C}+\boldsymbol{A}+\boldsymbol{Q})\psi = \boldsymbol{F}+\boldsymbol{G} \tag{39}$$

where

$$C_{(J,l),(I,k)} = \sum \int_\tau D_{lk}\frac{\partial N_I}{\partial x_i}\frac{\partial N_J}{\partial x_i}dx \tag{40}$$

$$A_{(J,l),(I,k)} = \sum \int_\tau a_{lk}N_I N_J dx \tag{41}$$

$$Q_{(J,l),(I,k)} = \sum \int_{\partial\tau} q_{lk}N_I N_J ds \tag{42}$$

$$F_{(J,l)} = \sum \int_\tau f_l N_J dx \tag{43}$$

$$G_{(J,l)} = \sum \int_{\partial\tau} g_l N_J ds \tag{44}$$

The sign Σ indicates the summation over all elements, and ψ is an N_pN-vector containing the numbers $\psi_{I,k}$

$$\psi = [\psi_{1,1}\psi_{2,1}\cdots\psi_{N_p,1}\psi_{1,2}\psi_{2,2}\cdots\psi_{N_p,2}\cdots\psi_{1,N}\cdots\psi_{N,N}]^T \tag{45}$$

The solution of Eq. (39) results in a set of nodal flux values for each neutron energy group in the domain of interest.

Two-Dimensional Model

The source, detector and surrounding soils were modeled in an axisymmetric geometry as shown in Fig. 4. This geometry is a reasonable representation of the physical arrangement of modern neutron moisture gauges. The volume of the soil shown in Fig. 4 exceeds the radius of influence of the neutron probe since the effective volume "sensed" by a neutron probe is approximately a sphere of radius 20 to 70 cm, increasing with decreasing moisture content (because at low water contents, the fast neutrons have to travel greater distances to undergo scattering interactions and so become thermalized).

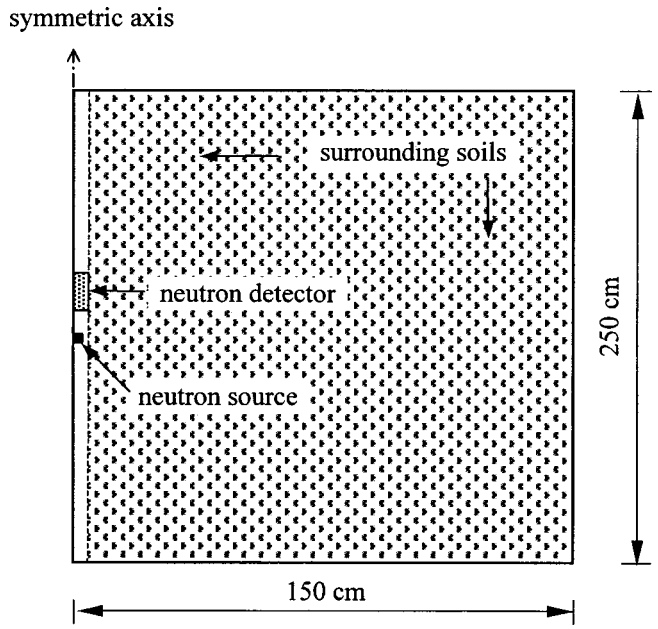

Fig. 4. Cylindrical system used for numerical analysis (not to scale)

The two-dimensional axisymmetric finite element analysis was carried out to calculate the thermal flux distribution in the system. A total of 4,073 three-node triangular elements were used in the analysis.

In order to include the effect of the detector in the analysis, the detector was treated as a separate region. The detector is usually a gas with a very large absorption cross section. The most widely used detector gasses are ^{3}He and $^{10}BF_3$. Their thermal absorption cross sections may be estimated from the following equation:

$$\sum_{a,D} = \frac{0.6023\times 10^{24}}{22.41\times 10^{3}} \frac{p}{760} \frac{273}{T_D} \frac{E}{100} \frac{\sqrt{\pi}}{2} \sigma_a^{2,200} \times 10^{-24} \sqrt{\frac{293}{T_n}} \ (\text{cm}^{-1}) \quad (46)$$

where p = pressure of the gas in the detector (in mm Hg); T_D = detector temperature (in degrees kelvin); E = percentage of the detector gas in the detector; and T_n = neutron temperature. For the $^{10}BF_3$-filled and ^{3}He-filled proportional counters, $\sigma_a^{2,200}$ may be taken as 3,813 and 5,330 barns, respectively.

It should be noted that the effects of the access tube and absorption in the neutron source are not taken into account in this study. Although the numerical approach described here could include these effects, it is believed that their influences on neutron flux at the detector are insignificant (at least for the aluminum access tubes considered here).

Once the distribution of the thermal neutron flux, ϕ_{th}, in the neutron detector (as shown in Fig. 4) is known, the gauge response (i.e., the number of counts or neutrons detected in a given time) can be obtained by integrating $\phi_{th}\ \Sigma_{a,D}$ over the volume of the detector. That is, by evaluating

$$\text{CR} = \int_v \phi_{th} \cdot \Sigma_{a,D} \cdot T \cdot dv \quad (47)$$

where CR = count rate and T = count period in seconds.

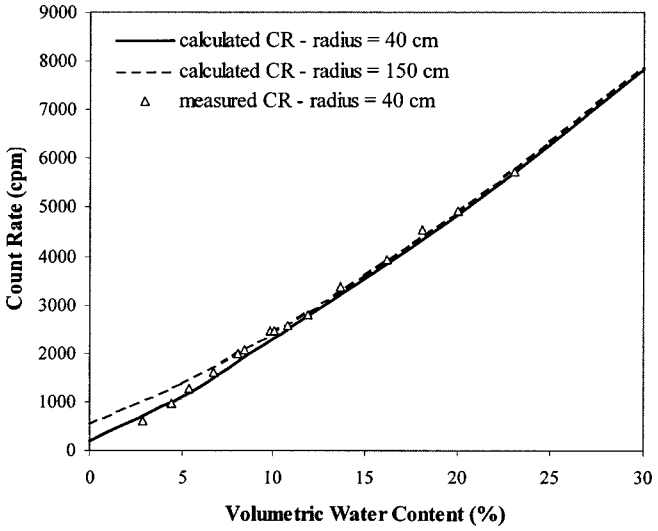

Fig. 5. Count rate as function of water volume percent for Borris soil—comparison of results predicted by numerical model with experimental results

Verification of Numerical Model Using Laboratory Experimental Results

In order to verify the validity of the seven-group neutron diffusion model, the numerical results were first checked against laboratory experimental results available in the literature.

The experimental data used for verification purposes were extracted from Olgaard (1965). Neutron probe experiments were conducted on different types of Danish soil by the Agricultural Department at the Riso Establishment, Roskilde, Denmark. Measurements were performed in a steel drum that was 80 cm in diameter and 100 cm in height. For each soil type, measurements were carried out at different water contents. Using the soil elemental composition given in Olgaard (1965), the count rates as function of water volume percent for Borris soil were predicted by the numerical model. It is noted that Borris soil is described as a ''loamy sand'' type of soil. The actual source-detector geometry of the Danish study (i.e., a source situated at the midline and just outside the detector) was used in the analysis. The source strength was 79,000 neutrons per second. The results are plotted against the experimental data in Fig. 5. As can be seen from Fig. 5, when the radius of the cylindrical system in the numerical model (see Fig. 4) was reduced from 150 to 40 cm, the predicted count rates agreed very well with the measured values. It is interesting to note that for water contents less than approximately 8%, the calculated count rates are larger than the experimental values. The reason for the discrepancy is that the size of the drum container used in the experiments was too small to prevent neutron leakage out of the container. Similar conclusions about neutron leakage in small-diameter containers at low water contents have been also reported by other researchers (Olgaard 1965; Olgaard and Haahr 1967; Elder and Rasmussen 1994).

Verification of Numerical Model Using Field Experimental Results

Soil and Site Description

The site selected for a field study is located on grassed rangeland some 10 km west of the city of Newcastle, Australia. The soil

Table 4. Composition of Dried Maryland Soils by Mass Percent

Element	Depth = 0.45 m	Depth = 1.25 m
H	0.30000	0.38000
Li	0.00166	0.00167
B	0.00600	0.00480
C	0.64000	0.41000
N	0.09000	0.12000
O	54.17000	52.51000
Na	0.32000	0.56000
Mg	0.50000	0.55000
Al	8.26000	8.64000
Si	30.87000	30.20000
P	0.01300	0.01300
S	0.09000	0.09000
Cl	0.00500	0.04600
K	1.21000	2.06000
Ca	0.04000	0.03000
Ti	0.37000	0.37000
Mn	0.00500	0.00500
Fe	3.10000	4.10000
Co	~0.00000	~0.00000
Cd	~0.00000	~0.00000

profile across the site is relatively uniform and can be generally described as 250 mm silty clay topsoil underlain by high plasticity clay to a depth of approximately 1.2 m, then a medium plastic silty clay to approximately 1.8 m, where highly weathered siltstone is encountered. The Maryland site classification for reactivity following the Australian Standard for Residential Slab and Footings (AS 2870 1996) is H (i.e., highly reactive, with a predicted open uncovered ground movement ranging between 40 and 70 mm). The instrumentation installed at the site includes: automatic weather station, surface movement probes, subsurface movement probes, neutron probe, gypsum blocks, in situ filter paper devices, thermocouples, and piezometers. Detailed description of the testing site can be found in Fityus et al. (2003).

Chemical Composition of Maryland Soils

In order to carry out the numerical analysis, it is necessary to first know the elemental composition of the soil with depth. A total of 14 chemical analyses of the soils at different depths over a 3 m interval were carried out. Before the analysis, the soil samples were dried at 105°C. Typical results of the chemical analyses for two depths are listed in Table 4. The list shows the mass percent of each element. It should be noted that the oxygen content in Table 4 was estimated by subtracting the sum of the percentages of all other elements from 100.

As can be seen from Table 4, about half the elemental weight is oxygen (which occurs as metal and silicon oxides). Oxygen is thus the main contributor to the scattering cross section (other major contributors are Si, Al, and Fe).

The macroscopic scattering and absorption cross sections are calculated from the elemental composition of the soil. The calculation involves a summation of microscopic cross sections over all elements in the soil.

Neutron Instruments

The neutron probe used in this study is a Campbell Pacific Nuclear Model 503 Hydroprobe. Fast neutrons are generated by the probe using a 50 mCi (1.85 GBq) Americium-241-Beryllium source, with a strength of 111,000 neutrons per second. A helium-3 filled proportional counter detector of 13.2 cm in length and 2.54 cm in diameter is used to detect thermalized neutrons. The neutron source is situated 3 cm below the detector. The commercial neutron probe was not modified in any way for the research work described herein.

Access Tubes

Aluminum access tubes of 53 mm external diameter and 1.9 mm wall thickness were used in this study. Because of the low thermal cross section of aluminum ($\sigma_a = 0.23$ b and $\sigma_s = 1.4$ b, see Table 2), it was considered that aluminum casings would have little effect on the neutron flux. All access tubes are sealed at the bottom. When not in use, the top end of the tube is covered with a cap to prevent the ingress of rain and debris.

Field Measurement

In order to calibrate the neutron probe readings with volumetric moisture contents, the soil moisture contents need to be measured independently. To do this, thin-walled steel tubes, 120 mm in length and 48 mm in diameter, were used to obtain soil samples from the experimental site. Each tube had a sharpened outward-facing edge to allow easy penetration of the soil. To minimize disturbance, the thin-walled steel tubes were pushed into the soil at a constant penetration rate. After being removed from the ground, the ends of the thin-walled sample tube were wax sealed, and then immediately sealed in an air tight jar to maintain the soil moisture content. The soil volumetric and gravimetric moisture contents and the soil density were determined on each soil sample following standard geotechnical practices.

After the last sample was obtained, an aluminum access tube was installed in the center of the core. The neutron probe was then lowered in the tube and count rates were measured at the same depths where the soil samples had been recovered.

The neutron counts of 16-s duration were taken in this study. The counting time interval of 16-s was chosen because it gave sufficiently precise readings in acceptable period of time after comparison with 32-, 64-, and 256-s counts.

Comparison of Numerical and Field Experimental Results

The results predicted by the numerical model were compared with the field observations at the Maryland site. The test site, approximately 80 m × 25 m, was divided into five distinct zones for study: an open area, a naturally grassed, tree affected area, a 10 m × 10 m area with an unloaded flexible cover, and a 10 m × 10 m area covered by a loaded reinforced concrete slab. Since 1994, the soil moisture content has been monitored at these zones by the neutron probe method.

The numerical model was used to predict the neutron counts with depth for the open area, based on the system geometry defined in Fig. 4 and the chemical analysis of the soils at different depths. The soil bulk density and volumetric moisture contents were determined from the field measurement by the thin-walled steel tube method. The calculated count rate variation with depth is plotted in Fig. 6. It can be seen that very good agreement is obtained between the numerical analyses and the field measurements.

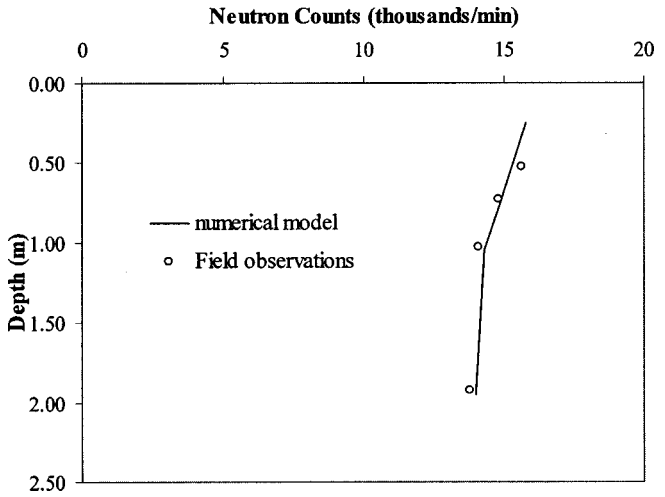

Fig. 6. Count rate variation with depth—comparison of results predicted by numerical model and Maryland field measurements

Conclusions

In this study, a numerical model based on multigroup diffusion theory has been developed to predict the neutron flux distribution in a neutron probe system. Neutron counts predicted by the neutron diffusion model are found to agree favorably with the measured data at a field site. The numerical results also compare very well with the experimental results available in the literature. It is believed that a calibration between neutron counts and moisture content for soils (including unsaturated expansive soil) can be accurately estimated using the proposed numerical model with a minimum of experimental effort. The establishment of a calibration relationship requires that the chemical composition of the soil be determined, and the geometry of the source-detector system be known. The numerical analysis also indicates that large containers are necessary for laboratory calibration to prevent neutrons leaking into the air surrounding the container, and so may be of assistance for laboratory calibration procedures.

An apparent disadvantage of the numerical model is the requirement of a complete elemental analysis of the soil. However, this analysis is now comparatively straightforward using modern analytical chemical methods (e.g., using high-resolution inductively coupled plasma mass spectrometry, HR-ICPMS), and is much easier than performing an experimental calibration on soils.

This research has shown that the proposed numerical model is capable of describing the response of a neutron moisture gauge to a degree of sophistication that has not been achieved previously. It is believed that the utilization of a model such as the one described here can lead to a much better understanding of the distribution of neutron flux in a neutron probe system for any geometry and soil type under a variety of environmental conditions. This greater capacity for interpretation of probe data may open up new applications for the neutron probe. For example, it may be possible to use the neutron probe to monitor rising salt (i.e., sodium chloride) in a groundwater system.

Acknowledgment

This research has been carried out with financial support from the Mine Subsidence Board of New South Wales.

References

AS 2870. (1996). ''Residential slab and footings-construction.'' Standards Australia, Sydney.

Bell, J. P., and McCulloch, J. S. C. (1969). ''Soil moisture estimation by the neutron method in Britain.'' *J. Hydrol.*, 7, 415–433.

Carneiro, C., and Jong, E. D.E. (1985). ''In situ determination of the slope of the calibration curve of a neutron probe using a volumetric technique.'' *Soil Sci.*, 139(3), 250–254.

Chanasyk, D. S., and Naeth, M. A. (1996). ''Field measurement of soil moisture using neutron probes.'' *Can. J. Soil Sci.*, 76, 317–323.

Dickey, G. L. (1990). ''Factors affecting neutron gauge calibration.'' *Proc., National Conf. ASCE Irrigation and Drainage Division*, ASCE, New York, 9–20.

Elder, A. N., and Rasmussen, T. C. (1994). ''Neutron probe calibration in unsaturated tuff.'' *Soil Sci. Soc. Am. J.*, 58, 1301–13071.

Fityus, S. G., Smith, D. W., and Allman, M. A. (2003). ''An expansive soil test site near Newcastle.'' *J. Geotech. Geoenviron. Eng.*, in press.

Gibson, W. M. (1980). *The physics of nuclear reactions*, Pergamon, Oxford, England.

Glasstone, S., and Edlund, M. C. (1957). *The elements of nuclear reactor theory*, D. Van Nostrand Company, Princeton, N.J.

Greacen, E. L. (1981). *Soil water assessment by the neutron method*, CSIRO Publication, East Melbourne, Victoria, Australia.

Haahr, V., and Olgaard, P. L. (1965). ''Comparative experimental and theoretical investigations of the neutronic method for measuring the water content in soil.'' *Symposium on the Use of Isotopes and Radiation in Soil-Plant Nutrition Studies, Ankara, Turkey, IAEA, Vienna, Austria, 129–147.*

Hughes, D. J., and Schwartz, R. B. (1958). *Neutron cross sections BNL-325*, Brookhaven National Laboratory, N.Y.

Iliffe, C. E. (1982). *An introduction to nuclear reactor theory*, Manchester University Press, Manchester, England.

International Atomic Energy Agency (IAEA). (1970). *Neutron moisture gauges: A guide-book on theory and practice*, International Atomic Energy Agency, Vienna, Austria.

Isbin, H. (1963). *Introduction to nuclear reactor theory*, Reinhold, N.Y.

Morris, P. H., and William, D. J. (1990). ''Generalized calibration of a nuclear moisture/density depth gauge.'' *Geotech. Test. J.*, 13, 24–35.

Mughabghab, S. F., Divadeenam, M., and Holden, N. E. (1981). *Neutron cross sections, Vol. 1, Part A.*, Academic, N.Y.

Olgaard, P. L. (1965). ''On the theory of the neutronic method of measuring the water content in soil.'' *Riso Rep. No. 97*, Danish Atomic Energy Commission, Copenhagen, Denmark.

Olgaard, P. L., and Haahr, V. (1967). ''Comparative experimental and theoretical investigations of the DM neutron moisture probe.'' *Nucl. Eng. Des.*, 5, 311–324.

Rawls, W. J., and Asmussen, L. E. (1973). ''Neutron field calibration for soils in the Georgia coastal plain.'' *Soil Sci.*, 116(4), 262–265.

Robinson, G. S., and Harrington, B. V. (1998). ''AUS98—The 1998 version of the AUS modular neutronics code system, ANSTO/E734.'' Australian Atomic Energy Commission, Research Establishment, Lucas Heights, New South Wales, Austrailia.

Schmugge, T. J., Jackson, T. J., and McKim, H. L. (1980). ''Survey of methods for soil moisture determination.'' *Water Resour. Res.*, 16(16), 961–979.

Silvestri, V., Sarkis, G., Bekkouche, N., Soulie, M., and Tabib, C. (1991). ''Laboratory and field calibration of a neutron depth moisture gauge for use in high water content soils.'' *Geotech. Test. J.*, 14(1), 64–70.

Stacey, W. M. (2001). *Nuclear reactor physics*, Wiley, New York.

Stone, J. F. (1990). ''Neutron physics considerations in moisture probe design.'' *Proc., National Conf. ASCE Irrigation and Drainage Division*, ASCE, New York, 1–8.

Vachaud, G., Royer, J. M., and Cooper, J. D. (1977). ''Comparison of methods of calibration of a neutron probe by gravimetry or neutron-capture model.'' *J. Hydrol.*, 34, 343–356.

Weinberg, A. M., and Wigner, E. P. (1958). *The physical theory of neutron chain reactors*, University of Chicago Press, Chicago.

Zweifel, P. F. (1973). *Reactions physics*, McGraw-Hill, New York.